International Scientific Colloquium
Modelling for Electromagnetic Processing
Hannover, October 27-29, 2008

Optimal Parameters of One-side Traveling Field Inductors for Stirring and Pumping Applications

V. Fireţeanu, M. Popa, S. Paşca

Abstract

This paper deals with the evaluation of optimal parameters of one-side linear flat travelling field inductors for stirring and pumping. It is proved that optimal design of such systems must corelate the electric conductivity of the stirred/pumped liquid with inductor pole pitch length, inductor and bath/channel width, airgap thickness and frequency.

Introduction

An important number of existing and potential applications of liquid driving by the action of electromagnetic forces, whose main advantage is the absence of mobile pieces in contact with the liquid, use one-side linear flat inductors of travelling field type. Based on analytical and finite element models, optimal values of main parameters of such inductors can be defined and evaluated.

1. Analytical model of the travelling field diffusion in the solid conductor half space

A magnetic field time (t) and space (x) dependent, expressed by formula $B(t,x) = B_m \cos(\omega t - 2\pi x/\lambda)$, where $\omega = 2\pi f$, f is the frequency, $\lambda = 2\tau$, τ is the pole pitch length of the inductor, is called *traveling magnetic field*. Such a field wave is generated by a *linear flat traveling field inductor*, characterized by a plane active face z = 0, Fig. 1.

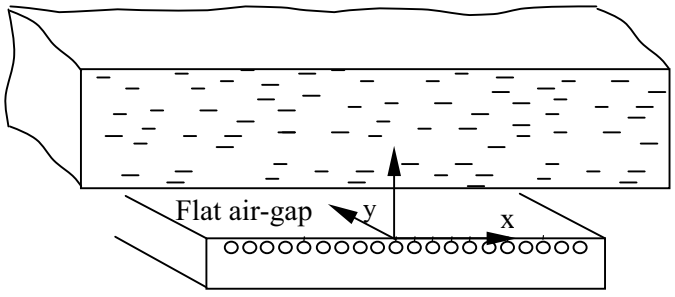

Fig, 1. Linear flat inductor for electromagnetic stirring

The parameter *penetration depth of traveling field* characterizes the decrease of field quantities inside a half space of solid conductor type. The *driving force component* is the component of the electromagnetic force oriented along x coordinate, Fig. 1. The *levitation component* is oriented along z coordinate.

The simplified analytical model of traveling field diffusion presented in this section is based on the following assumptions:

- there is no air gap, the active face of the inductor is the bottom of the bath;
- the inductor and the bath are extended to infinity along the coordinates x and y, Fig. 1;
- the depth of the bath, region having the conductivity σ and the permeability μ_0, is much higher than the penetration depth of traveling field;

- the magnetic core is ideal, without slots, nonconductive and with infinite permeability.

The inductor winding is modeled by a current sheet in the plane z = 0, Fig. 1. The structure of the current sheet density is $\mathbf{J}_s$ [0, $J_s(x,t)$, 0] , where $J_s(x,t) = J_{sm}\cos[\omega t - (\pi/\tau)x]$.

The current density in the bath has the structure **J** [0, J(x,z,t), 0], the magnetic vector potential, defined by the formula **B** = curl **A,** is oriented along the same axis, **A** [0, A(x,z,t), 0] and the vector of magnetic flux density has the structure **B** [$B_x(x,z,t)$, 0, $B_z(x,z,t)$].

The unknown A(x,z,t) satisfies the equation:

$$\frac{\partial^2 A}{\partial x^2} + \frac{\partial^2 A}{\partial z^2} = \mu_0 \sigma \frac{\partial A}{\partial t} \tag{1}$$

The two boundary conditions:

$$H_x(x,0,t) = \frac{B_x}{\mu_0} = -\frac{1}{\mu_0}\frac{\partial A}{\partial z} = J_s \quad \text{and} \quad A(x,\infty,t) = 0 \tag{2}$$

express the known value of the magnetic field at the interface between the magnetic core and the bath and the property of field vanishing to infinity of z coordinate, Fig.1.

The complex image $\underline{A}(z)$ of the magnetic potential, defined by the transformation $A(t,x,z) = \text{Real}\{\underline{A}(z)\cdot\exp[j(\omega t - \pi x/\tau)]\}$, is $\underline{A} = (\mu_0 J_{sm}/\underline{\gamma})e^{-\underline{\gamma}z}$, where $\underline{\gamma} = [(\pi/\tau)^2 + j\omega\mu_0\sigma\}]^{0.5}$. The complex images of the electromagnetic field quantities are:

$$\underline{B}_x = \mu_0 J_{sm}\, e^{-\underline{\gamma}z}, \quad \underline{B}_z = -\,j(\pi/\tau)(\mu_0 J_{sm}/\underline{\gamma})\, e^{-\underline{\gamma}z}, \quad \underline{J} = -\,(j\omega\mu_0\sigma J_{sm}/\underline{\gamma})\, e^{-\underline{\gamma}z} \tag{3}$$

The modulus of these quantities varies with respect the coordinate z as follow:

$$B_x = \mu_0 J_{sm}\, e^{-z/\delta}, \quad B_z = (\pi/\tau)(\mu_0 J_{sm}/\gamma)\, e^{-z/\delta}, \quad J = (\omega\mu_0\sigma J_{sm}/\gamma)\, e^{-z/\delta} \tag{4}$$

where γ is the modulus of $\underline{\gamma}$ and $\delta = 1/\text{Real}(\underline{\gamma})$ is the *penetration depth of the traveling field.*

The penetration depth that characterize the decrease of the field inside the bath has the expression $\delta = (\tau/\pi)\{2/[(1+\varepsilon^2)^{0.5}+1]\}^{0.5}$, where the $\varepsilon = \omega\mu_0\sigma/(\pi/\tau)^2 = v_s l_c/[1/(\mu_0\sigma)]$ is called *Reynolds magnetic number*. This number is function of travelling wave velocity $v_s = 2f\tau$, characteristic length $l_c = \tau/\pi$ and magnetic viscosity $1/(\mu_0\sigma)$.

For reduced conductivity σ and/or frequency f and/or pole pitch τ, i.e. $\omega\mu_0\sigma << (\pi/\tau)^2$ respectively $\varepsilon << 1$, the approximation of penetration depth, $\delta \approx (\tau/\pi)$, is independent on σ and f. Consequently, a <u>good penetration of the traveling field implies high values of</u> τ. The field spatial structure, Fig. 2a, depends only on τ and is independent on σ and f.

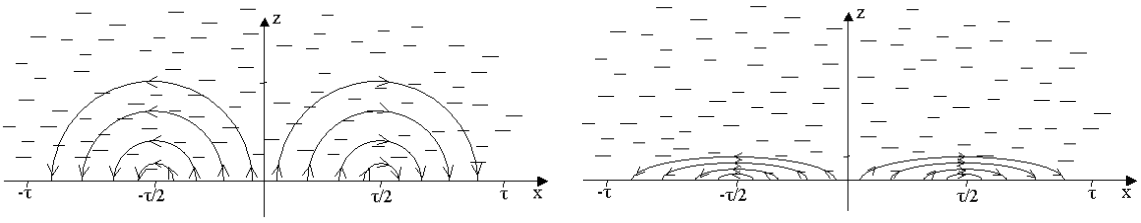

a) $\varepsilon << 1$ b) $\varepsilon >> 1$

Fig. 2. Penetration of traveling magnetic field

For values of f and τ leading to $\omega\mu_0\sigma >> (\pi/\tau)^2$, respectively for $\varepsilon >> 1$, the approximation of penetration depth $\delta \approx [2/(\omega\mu_0\sigma)]^{0.5}$ is independent on τ. In this case a <u>good penetration of the traveling field implies reduced values of frequency</u>. The field penetration, Fig. 2b, depends on σ and f and is independent on τ.

The vector of electromagnetic force density concerns the driving component f_x, oriented along the direction x of traveling field, and the levitation component f_z, normally oriented with respect the face of the inductor. If $\varepsilon >> 1$ the component f_z is greater than f_x, and if $\varepsilon << 1$ the component f_z is negligible with respect f_x. For $\varepsilon = 2\sqrt{2}$, $f_z = f_x$.

The integral of force densities from z = 0 to infinity gives the total driving force F_x and levitation force F_z related to the unit of surface in (xy) plane. The equation $\partial F_x/\partial\varepsilon = 0$ gives the optimum value $\varepsilon_o = \sqrt{3}$, for which the driving force is maximum.

The ratio between the force F_x and the active power P_J generated by the current induced in the bath is $F_x/P_J = 1/v_s = 1/(2f\tau)$. Consequently, an efficient stirring, characterized by high driving force and reduced active power, implies reduced values of frequency.

2. Influence of frequency, number of winding phases and inductor pole pitch length

The results of two 2D finite element models, for a two-phase (m = 2) and for a three-phase (m = 3) four poles inductor, correspond to the rms value of the current sheet, $J_{sm}/\sqrt{2}$ = 100 A/mm, air gap thickness 100 mm, the resistivity of the bath 0.2510^{-6} Ωm and pole pitch length 360 mm. The winding of the two-phase inductor is placed in 18 slots and the phase of currents in the successive coils is 0_-90_180_90_0_-90_180_90 degrees. The winding of the three-phase inductor is placed in 24 slots and the phase of currents in successive coils is 0_-60_-120_-180_120_60_0_-60_-120_ -180_120_60 degrees. All global results correspond to 300 mm width of the inductor and bath.

The graphical results in the Figs. 3, 4 correspond to the two-phase application.

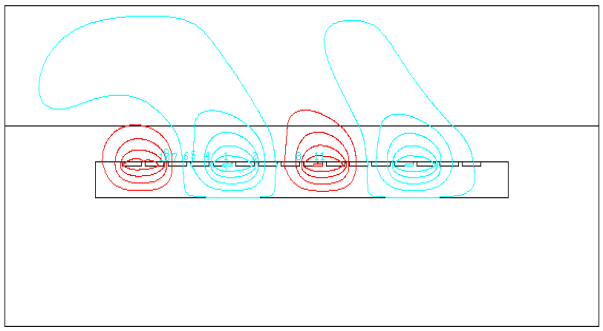

Fig. 3. Lines of magnetic field

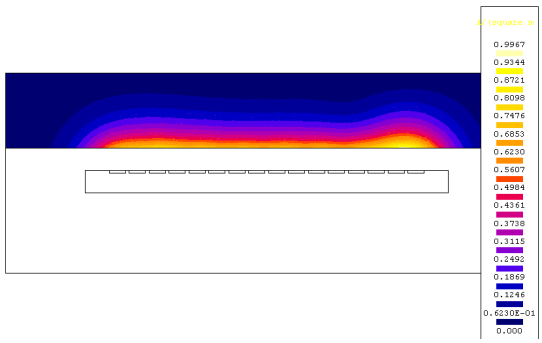

Fig. 4. Module of induced current density

The dependences on frequency of the driving force F_x , Fig. 5, show as optimal value of frequency, f_o = 7 Hz, corresponding to the maximum of driving force. The maximum of driving force for m = 3 is greater with (395.3 – 353.3)/353.3 x 100 = 11.9 % than for m = 2.

Unlike the driving component, the levitation component F_z, Fig. 6, and the power induced in the bath, Fig. 7, continuously increases when the frequency increases. The two components of the force are equal for the frequency f_e = 3.81 Hz, value under which the driving force is greater than the levitation force.

When the frequency increases the gradient of the electromagnetic force diminishes more than the gradient of the induced power. Consequently, low values of frequency must be considered for efficient driving applications in traveling magnetic fields.

The results in the Table 1 concern the optimal frequency f_o corresponding to maxim of driving force, the stirring force F_{xL}, levitation force F_{zL} and active power P_{J2L} related to the unit inductor length and the field penetration depth δ in the bath. The comparison shows:

(1) if the pole pitch length increases, the value of optimal frequency f_o decreases;

(2) if the pole pitch length increases, the efficiency of the bath stirring, expressed by the the ratios F_{xL}/P_{J2L} and F_{zL}/P_{J2L} , increases.

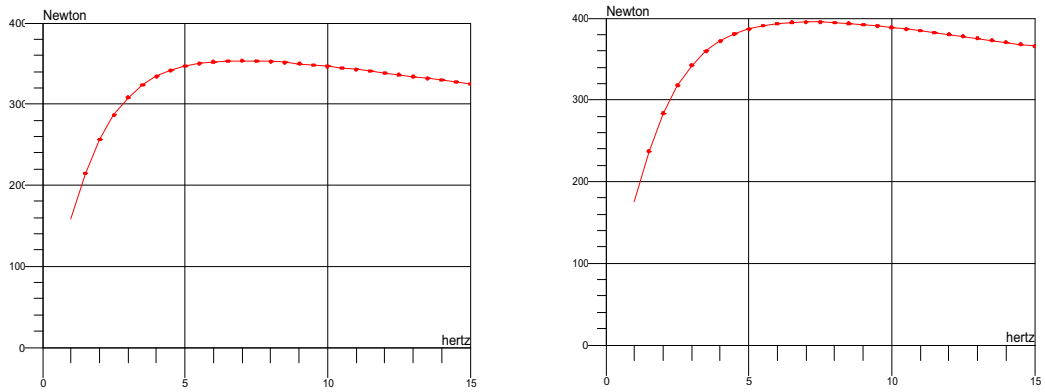

m = 2 m = 3

Fig. 5. Dependence on frequency of stirring component F_x the electromagnetic force

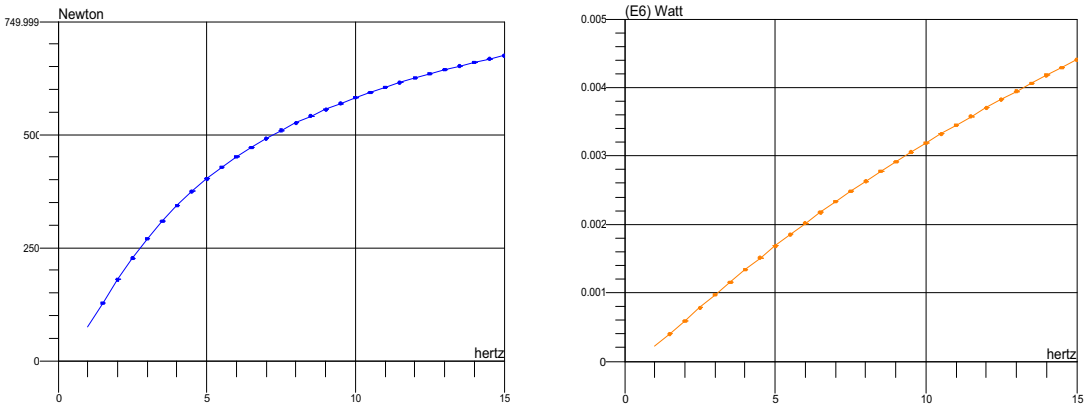

Fig. 6. Levitation force F_z and the active power induced in the bath (m = 2)

Table 1. Results for different values of inductor pole pitch length (for m = 2)

τ [mm]	f_o [Hz]	F_{xL} [N/m]	F_{zL} [N/m]	P_{2L} [W/m]	δ [mm]	F_{xL}/P_{2L} [N/W]	F_{zL}/P_{2L} [N/W]
254.6	14.5	132.02	209.07	1380.5	56.8	0.096	0.631
360.0	7.00	243.26	341.08	1618.8	80.3	0.150	0.713
509.1	3.01	379.66	437.79	1455.7	119.3	0.261	0.867

3. Evaluation of optimal frequency based on 3D finite element models

The 2D models represent a good enough approximation of the devices for stirring and pumping in traveling field only if the width of the inductor and bath is much more higher than the pole pitch length. In many practical applications this is not the case, and consequently the 3D finite element analyses becomes compulsory.

The application studied in this section consider a two poles three-phase inductor, Fig. 7, with the pole pitch length 528 mm, composed of 12 coils around a magnetic core whoose width is 350 mm.

3.1. *Stirring model*

Figure 8(a) contains three regions of the finite element computation domain in case of a stirring application in traveling field - the magnetic core of the inductor, a non magnetic and conductive protection plate of 5 mm thickness, placed at 20 mm distance from the inductor, and the aluminum bath having the width 400 mm, placed at 125 mm distance from the inductor. A three-phase symmetrical system of currents sypply the inductor, whose winding is star connected; the density of the inductor current sheet is 154.91 A/mm.

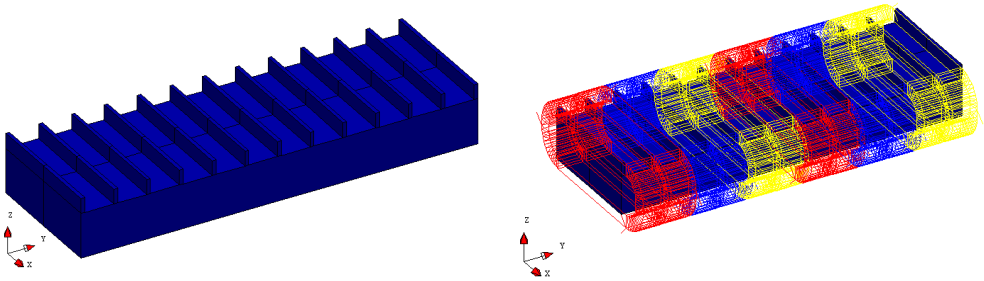

Fig. 7. One side traveling field flat inductor

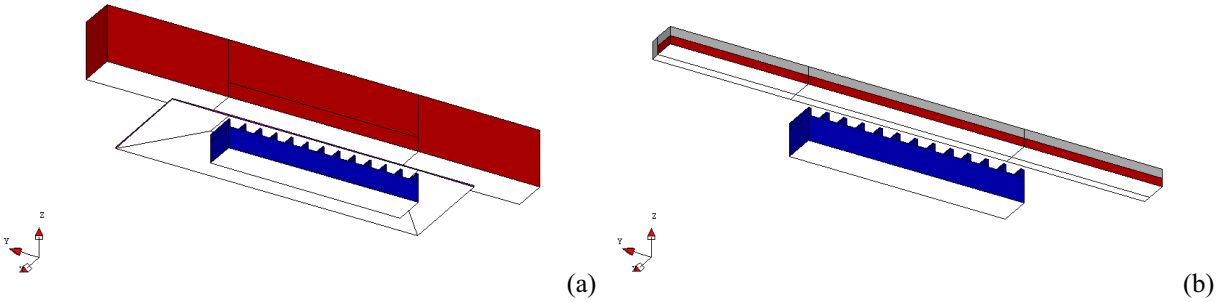

(a) (b)

Fig. 8. Regions of the computation domain – stirring model (a), pumping model (b)

The numerical results in Table 2 reflect the dependence on supply frequency of the driving force $F_{y,}$ levitation force F_z, power induced in the bath P_{Al} and in the protection plate P_{pp} and the total active power of the inductor P, which includes the Joule losses in the inductor coils. The optimal value of frequency is around 7 Hz, and the comparative analysis of the results confirm the interest for low values of the frequency.

Table 2. Stirring model results

f [Hz]	F_y [N]	F_z [N]	P_{Al} [kW]	P_{pp} [kW]	P [kW]
3	701.5	577.7	2.906	0.535	47.35
5	792.2	844.8	5.317	1.393	50.63
7	804.6	1193.3	7.429	2.601	53.91
9	792.8	1370.0	9.320	4.151	57.38
12	763.1	1554.2	11.841	7.099	62.81
20	683.5	1830.0	17.429	18.504	79.81

The chart of the volume density of the stirring component of the electromagnetic force for two values of the frequency, Fig. 9, show the driving action of the electromagnetic field is located more and more toward the botom of the bath when the frequency increases. Since the velocity of the liquid bath vanish toward the botom, supposing the same value the driving force for two different values of frequency (for example 5 Hz and 9 Hz, see Table 2), a higher intensity of the stirring is waited for the frequency 5 Hz.

3.1. *Pumping model*

Figure 8(b) contains three regions of the computation domain in case of a pumping application in traveling field - the magnetic core of the inductor, the refractory walls of the pumping channel and the liquid aluminum inside the channel, having the width 230 mm and the thickness 45 mm, placed at 125 mm distance from the inductor. A three-phase

symmetrical system of currents sypply the inductor, whoose winding is star connected; the density of the inductor current sheet is 145.45 A/mm.

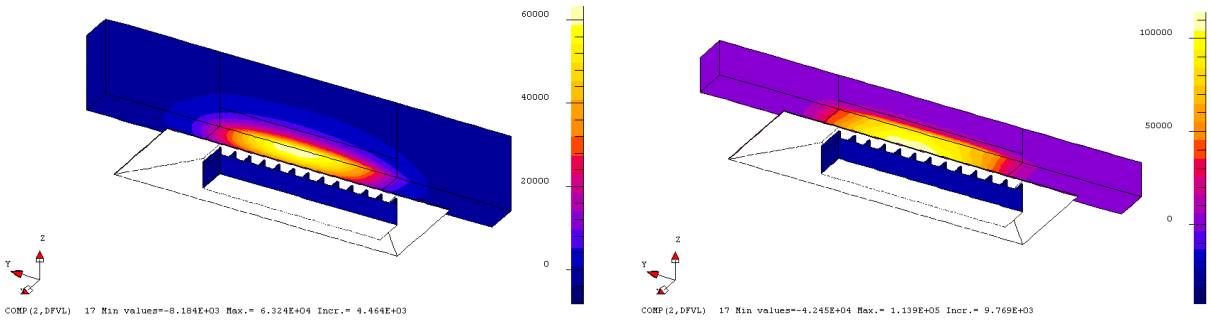

f = 3 Hz f = 20 Hz

Fig. 9. Chart of driving force density for two frequencies

The results in Table 3 reflect the dependence on supply frequency of the pumping force F_y and power induced in the aluminum P_{Al} . The value of frequency for which the pumping effect is maximum, f = 30 Hz , is much higher than the optimum value for stirring.

Table 3. Pumping model results

f [Hz]	F_y [N]	P_{Al} [kW]
7	224.3	2.16
12	334.8	5.52
15	377.7	7.77
20	417.7	11.4
30	429.6	17.6
40	409.0	22.3
50	393.8	26.1

Conclusions

The optimal design of the one-side traveling field inductors for electromagnetic stirring or pumping applications must corelate the electric conductivity of the stirred/pumped liquid with inductor pole pitch length, inductor and bath or channel width, airgap thickness and inductor supply frequency.

For given values of conductivity, airgap thichness, pole pitch length, inductor and bath width, channel cross-section, there are for both applications optimal values of the frequency with respect the driving force.

References

[1] Khristinich, R.M., Timofeyev, V.N., Stafieskaya, V.V., Velenteyenko, A.V.: *Molten Metal Electromagnetic Stirring in Metallurgy*. Proceedings of International Scientific Colloquium **Modelling for Electromagnetic Processing**, Hannover, March 24-26, 2003

[2] Gelfgat, Yu., Mikelsons, A., Krumins, J., Pedchenko, A.: *On the Transversal End Effect in the Linear Induction Pump with Large Non-magnetic Gaps*. Proceedings of International Scientific Colloquium **Modeling for Electromagnetic Processing**, Riga, June 8-9, 2008

Authors

Prof. Dr.-Ing Fireteanu, Virgiliu
Faculty of Electrical Engineering
POLITEHNICA University of Bucharest
313 Spl. Independentei
RO-060042 Bucharest, Romania
E-mail: firetean@amotion.pub.ro

Prof. Dr.-Ing. Popa, Monica and Prof. Dr.-Ing. Pasca, Sorin
Faculty of Electrical Engineering and Information Technology
University of Oradea
1, Universitatii
RO- Oradea, Romania
E-mail: spasca@uoradea.ro